Mechanical Testing and Diagnosis
ISSN 2247 – 9635, 2012 (II), Volume 3, 44-54

WEAR INVESTIGATION OF ROUGH BODIES IN CONTACT UNDER PARTIAL SLIP CONDITIONS

George GAVRILĂ, Spiridon CREŢU

"Gheorghe Asachi"Technical University, Faculty of Mechanical Engineering, Iași, ROMANIA

george_gavrila@yahoo.com

ABSTRACT

The paper presents a numerical model to investigate wear under partial slip conditions for smooth and rough contacting bodies. The wear simulation is based on the Archard wear law and is applied to a sphere on a flat geometry. In this numerical model, an analytical simulation of roughness is considered, which even for small magnitudes, is an important factor that cannot be neglected. The effect of an elastic perfectly-plastic material is also considered to limit the peaks of pressure on each contacting asperity.

Keywords: Roughness, wear, stick-slip, contact mechanics

1. INTRODUCTION

Wear of contacting surfaces is one phenomenon of the processes occurring in the contact interaction. Wear represents a progressive loss of material from the surfaces in contact due to their fracture in the friction interaction leading to a gradual change of dimensions and shape of the contacting bodies. Usually, the machines precision is affected by wear and as well, sometimes, the wear could lead to machine failure.

The main root cause of the wear is the friction between the contacting bodies. In general, in the formulation of contact problems, the friction is defined as a relation between the tangential and the normal stresses in the contact zone.

Considering a tangential force Q applied to the bodies and satisfying the condition $Q < \mu P$, where P is the normal force and μ is the coefficient of friction, then a partial slip occurs; this is characterized by the existence of the stick and slip zone within the contact region. This phenomenon is named the static friction. The contact problems with partial slip in contact region were considered by [3], [14], [16], [13], [10], etc. The solution of the problems includes the determination of the positions and sizes of the stick and slip zones for different given loading conditions. It is also shown that the area of the stick zones decreases and tends to zero if $Q \to \mu P$.

Mechanical Testing and Diagnosis, ISSN 2247 – 9635, 2012 (II), Volume 3, 44-54

Most recent studies are provided by [8] regarding the effect of dissimilar material constants and [18] for alternative contact geometries. As well, the Cattaneo-Mindlin model has been reviewed recently by [4, 5].

Having the partial slip problem solved and applying the Archard's wear law, it is possible to determine the fretting due to wear. Then, the contact surfaces are modified due to wear and, thus, the contact pressure. This cycle constitutes the basis for the contact profile and the wear evolution. [9] demonstrates that the contact pressure will be significantly different than the one predicted by the Herzian theory when using an updating algorithm considering the contact profile and the wear evolution.

An analytical model that evaluates the evolution of stress and the contact profile has been developed by [7] and they showed that an asymptote exists for the wear and the contact profiles. This model considered the elastic bodies and the smooth surfaces in contact.

[11] developed a numerical model considering a more complex boundary case: sinusoidal and statistical generated rough surfaces and elastic-perfectly plastic materials in contact.

This paper presents a simplified numerical model based on already developed analytical solutions in order to examine the pressure and the contact geometry for smooth and rough surfaces in contact and elastic perfectly-plastic materials.

2. ANALYTICAL FORMULATION

Figure 1 depicts a schematic of the configuration used in this model; two elastic bodies in contact, a ball in contact with an half space, subjected to a normal load P and an oscillating tangential force $Q(t)$ which acts in the interface plane X to avoid the creation of a moment in the contact zone.

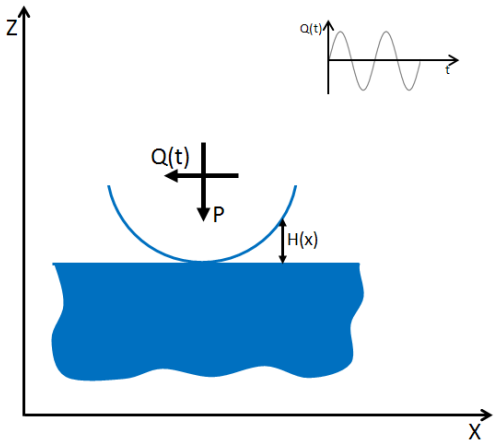

Fig. 1. Contact geometry

The partial slip condition is fulfilled, so $Q(t) \leq \mu P$, where P represents the normal load applied to the ball and μ the coefficient of friction, assumed to be constant.

Additionally, the following hypotheses are considered: the worn material is removed from the friction zone and the contacting bodies are modelled using the elastic-half space assumptions.

As well for the sake of simplicity, the roughness of both bodies is added to one body. Actually, at the beginning of the simulation, the roughness function is superimposed to the overlap function between the two bodies in contact.

2.1. Normal Pressure Distribution

Viewing that we are using the elastic-half space assumptions, the curvature of the two contacting bodies can be represented by an equivalent indenter and an elastic half space.

The governing equations in the analytical form used for the normal pressure problem, are given by [6]:

- the geometric equation of the elastic contact:

Mechanical Testing and Diagnosis, ISSN 2247 – 9635, 2012 (II), Volume 3, 44-54

$$g(x,y) = h(x,y) + w(x,y) - \delta_0 \quad (1)$$

- the integral equation of the normal displacement of the elastic-half space frontier:

$$w(x,y) = \frac{1}{\pi}\left(\frac{1-\upsilon_I^2}{E_I} + \frac{1-\upsilon_{II}^2}{E_{II}}\right) \times \iint_{A_r} \frac{p(\xi,\eta)}{\sqrt{(x-\xi)^2 + (y-\eta)^2}} d\,\xi d\eta \quad (2)$$

- the equilibrium equation:

$$\int_{A_r} p(x,y)dxdy = P \quad (3)$$

where, $h(x,y)$ is the overlap between the two surfaces in contact, $w(x,y)$ is the sum of the elastic normal displacement of the two surfaces in contact, δ_0 is the rigid displacement, E_I, E_{II} are the Young's modules of the two materials, $\upsilon_I, \upsilon_{II}$ are the Poisson's coefficients of the two materials, A_r is the real contact area and $p(x,y)$ is the pressure distribution obtained due to the application of the normal load P.

Additionally the following non-penetration and non-adherence conditions must be fulfilled:

$$g(x,y) = 0, p(x,y) > 0, (x,y) \in A_r \quad (4)$$

$$g(x,y) > 0, p(x,y) = 0, (x,y) \notin A_r \quad (5)$$

In order to solve the equations above (1-3), a discrete formulation is also available. The convolution product between the pressure p and the elastic response K is done using the DC-FFT method. Viewing that this is not the object of this paper, all the other details related to this numerical method can be found on [6].

2.2. Tangential Tractions Distribution

The Cattaneo-Mindlin problem is the case of two elastic bodies subjected to a normal load P and a tangential load $Q_x \leq \mu P$. According to the Coulomb law of friction, these two bodies are in equilibrium, meaning that there is no movement as gross sliding between them. [3] and then [15] demonstrated for Herzian geometries that the solution of the adhering tangential problem presents a singularity at the edges of the contact, which leads to an infinite shear.

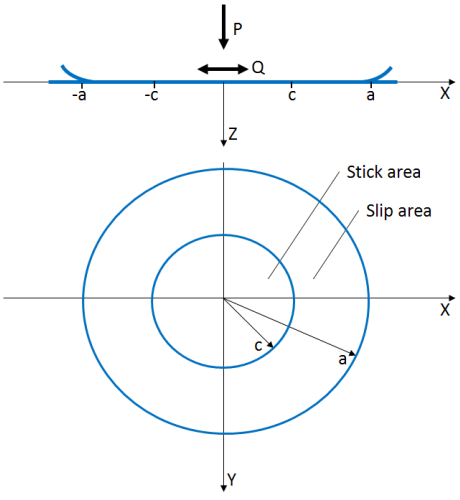

Fig. 3. A schematic sphere on plane contact

The slip invariably starts at the edge of each contact area and, following [3], the shear tractions are considered as the superposition of a full sliding component and a corrective part $q^*(x)$, non-zero only in the stick zone. The fully sliding component is given by the simple multiplication of the pressure distribution by the coefficient of friction.

The fully sliding shear traction distribution is given by [10]:

$$q(x,y) = \mu p(x,y) \quad (6)$$

The partial slip tractions are then calculated by introducing a corrective traction term $\mathbf{q}^*(\mathbf{x})$ as:

$$q(x,y) = \mu p(x,y), x \in S_{slip} \quad (7)$$

$$q(x,y) = \mu p(x,y) + q^*(x,y), x \in S_{stick} \quad (8)$$

Mechanical Testing and Diagnosis, ISSN 2247 – 9635, 2012 (II), Volume 3, 44-54

The stick zone for a smooth circular contact is located at the center of the Hertzian contact. For a spherical indenter on an elastic half space (Fig. 3), the stick zone radius c can be obtained from Johnson in 1985 [10]:

$$\frac{c}{a} = \sqrt[3]{1 - \frac{Q}{\mu P}} \tag{9}$$

Analytical expressions for sliding are also given by Goryacheva et al., in 2001 [7]. The component on *Y* direction exists due to the coupling between the tangential contributions but, usually, is neglected. The relationships to be considered are:

$$s_x = \begin{cases} 0, if\ x < c, \\ (u_{x1} - u_{x2}) - \delta_x, if\ c < x < a, \end{cases} \tag{10}$$

$$s_y \approx 0 \tag{11}$$

where, u_{x1} and u_{x2} are the tangential displacements of the contact surfaces at the point x, δ_x is the relative tangential displacement of the contact bodies, c is the size of the stick zone and a is the half width of the contact.

2.3. Surface Generation

In this numerical model an analytical simulation of roughness was considered by choosing a combination of sinus and cosines functions [6]. The frequency of these two functions can be different on *X* and *Y* directions. The following relationship is available:

$$R_{ij} = A \times cos\left(\frac{\pi}{2} \times A \times y_j \times tan\left(\theta_y\right)\right) \times sin\left(\frac{\pi}{2} + \frac{\pi}{2} \times A \times x_i \times tan(\right. \tag{12}$$

As already highlighted before, the roughness was superimposed on one body and the other one has been considered smooth. The parameters considered in the equation (12) have the following values: the amplitude $R_{max} = 0.2\mu m$, $\theta_x = 5.7^c$ considering the $x - O - x$ axis and $\theta_y = 1^c$ considering the $y - O - y$ axis.

2.4. Wear Evolution

After evaluating the pressure distribution and the shear tractions, wear is calculated using the method proposed by [7].

Archard's law [1] stays at the basis of different wear mechanisms and the following relation between the linear rate of wear, the contact pressure $p(x, t)$ and the rate of slippage $V(x, t)$ was proposed:

$$\frac{\partial w}{\partial t} = K_w p(x, t) V(x, t) \tag{13}$$

where K_w is the wear coefficient, which depends on the properties of the interacting bodies, the temperature, etc. In the problem in question, $V(x, t) = |\partial s(x, t)/\partial t|$, where the relative slippage $s(x, t)$ at the point x at the instant of time t.

The equation (13) can be written:

$$\frac{\partial w}{\partial t} = K_w p(x, t) |(\partial s(x, t))/\partial t| \tag{14}$$

The change in the shape of the surface during wear leads to a redistribution of the contact stresses.

It must be considered that, in a single cycle of variation of the shear force $Q(t)$, the shear stresses considerably change, as well as the relative slippage of the surfaces, and the size of the slip zone; at the same time, the contact pressures and the size of the contact area change only slightly. In the case of contacting bodies made of same materials, the shear

Mechanical Testing and Diagnosis, ISSN 2247 – 9635, 2012 (II), Volume 3, 44-54

stress distribution generally has no effect on the contact pressures and the size of the contact area.

To be noted that in the problem presented by [7] there are two scales of time. The first one is connected with the time of one cycle. During one cycle the redistribution of the shear contact stresses and the variation of the stick zone size take place as a feedback to the variation of the tangential force $Q(t)$. The contact shape variation is negligibly small in one cycle and it follows that the changes of the contact pressure and the contact width are also small in one cycle. The changes related to these values are linked with the second time scale, which is the number of cycles.

The value $\Delta w(x, N)$ denotes the wear increment of both bodies at the *N*th cycle. Thus, the wear after *N* cycles is calculated by:

$$w(x, N) = \sum_{n=1}^{N} \Delta w(x, n) \tag{15}$$

The overlap between the two contacting bodies is affected at each *N*th cycle by the quantity of wear calculated at that cycle. As shown above this quantity of wear depends directly on the pressure value and on the slip value on each surface point. So, if the overlap is noted $H(x, N)$, the governing equation to be considered at each iteration is given:

$$H(x, N) = H(x, N-1) + \Delta w(x, N) \tag{16}$$

2.5. Plastic Deformation

Viewing that into this model we considered rough surfaces with large number of asperities the contact pressure exceeds the elastic limit of most materials. In order to avoid these high peaks of pressure we assumed an elastic-perfectly plastic material. The pressure, is limited to a predetermined value of 4500 MPa. This value is calculated to be about three times the yield stress of the material, which correlates to the hardness strength of most materials.

3. RESULTS AND DISCUSSIONS

In this section, the results are obtained based on the following input parameters: $P = 50N$ (normal force), $Q = 20N$ (tangential force), $\mu = 0.5$ (coefficient of friction), $E = 208\ GPa$ (Young modulus), $\vartheta = 0.3$ (Poisson coefficient) and the wear coefficient $K_w = 7 \times 10^{-13} Pa^{-1}$ [17], which was held constant.

The results of the calculation of contact normal pressure are presented in Figs 4 and 5. The results indicate that the pressure essentially changes during the wear process. It increases within the stick zone and decreases inside the slip zones where wear occurs. The largest peak of pressure for a smooth surface occurs at the ends of the stick zone after the maximum numbers of cycles used on the model, in this case 30000 cycles.

In Fig. 4, there is no limitation of the high pressure peaks, where normally the contacting bodies are plastically deformed. This can be observed in the Fig. 6, where an elastic perfectly-plastic limit of 4500 MPa was imposed.

For the case of a rough surface, the simulation was done till 7000 cycles, due to the fact that after this number, in the slip area, the pressure and the slip values are almost the same, which will lead to a similar behaviour as for a smooth surface for any additional imposed wear cycle. This can be observed in Fig. 7. In the figure below, it can be observed that the normal pressure for a rough surface after 7000 cycles (the red line) is having the same values on the slip area as for a smooth surface after the same number of cycles.

Mechanical Testing and Diagnosis, ISSN 2247 – 9635, 2012 (II), Volume 3, 44-54

[7] predicted no change in the stick zone size as the number of cycles increases. But, as it can be seen as well in Fig. 7, due to the assumption of a plastic deformation, the edges of the stick zone deform due to the presence of very large pressures. This leads to a continuously reducing of the stick zone. The purple line from the graph (pressure after 30000 cycles) depicts this phenomenon. This observation was done as well by [11].

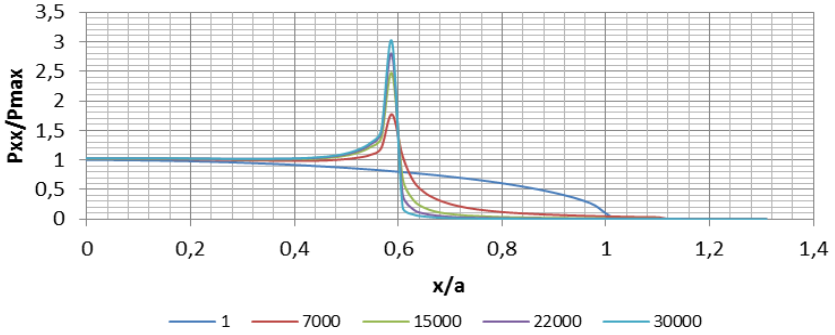

Fig. 4. Evolution of the normal pressure distribution due to wear for a smooth surface (2D half)

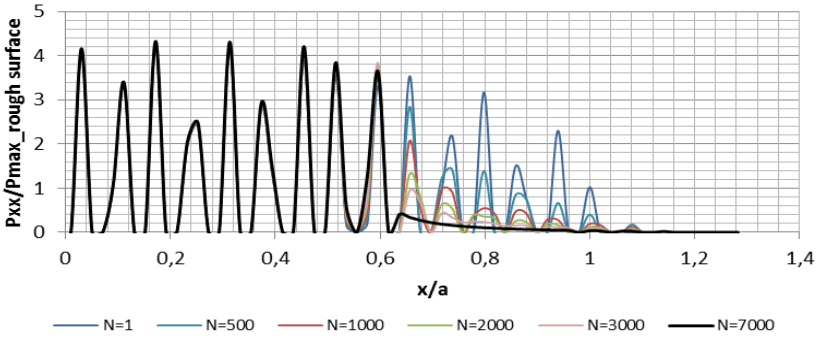

Fig. 5. Evolution of the normal pressure distribution due to wear for a rough surface (2D half)

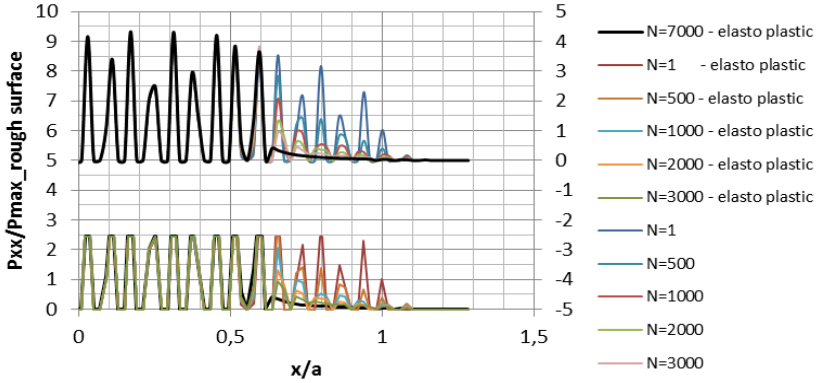

Fig. 6. Evolution of the normal pressure distribution due to wear for a rough surface (2D half). Comparison between elastic (top graph – right scale axis) and elastic perfectly-plastic material (bottom graph – left scale axis)

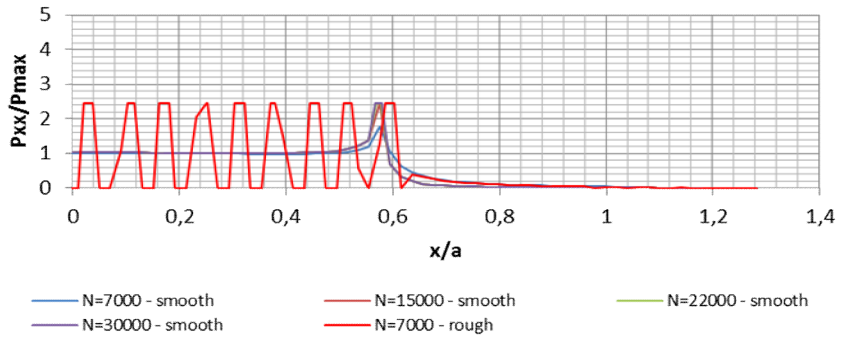

Fig. 7. Evolution of the normal pressure distribution due to wear (2D half) for a smooth and rough surface and elastic perfectly-plastic material behaviour

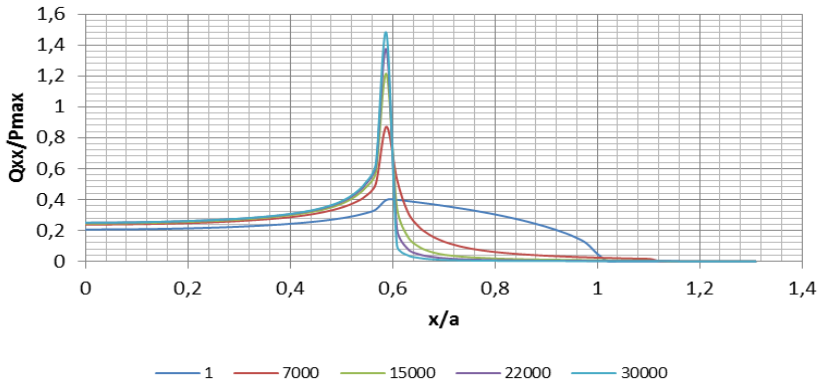

Fig. 8. Evolution of the shear tractions distribution due to wear for a smooth surface (2D half)

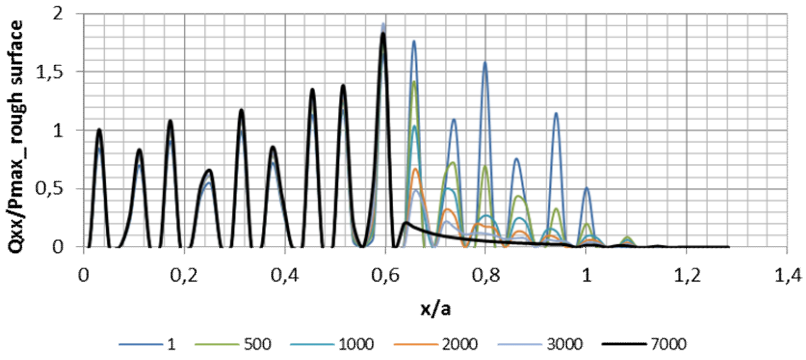

Fig. 9. Evolution of shear tractions distribution due to wear for a rough surface (2D half)

The shear tractions within the contact area exhibit a similar behaviour.

The evolution of the gap is presented in Figs 10 and 11. The maximum wear displacements take place in the middle points of the slip zones for both types of surface, smooth and rough.

Mechanical Testing and Diagnosis, ISSN 2247 – 9635, 2012 (II), Volume 3, 44-54

The wear during one cycle is directly proportional to the normal pressure and the slip function. This leads to the fact that the maximum wear value is in the middle of the slip zones. This area is the one supporting the highest wear phenomenon at the beginning of the wear process. This is valid for a smooth surface. In the case of rough surfaces, the wear takes place at first on the asperities where are located the biggest peaks of pressure. After a certain number of cycles (in the shown example, about 7000 cycles), the asperities on the slip area are worn, the material is removed and for the additional number of cycles the behaviour is similar as for a smooth contact.

After certain number of cycles, the wear value during one cycle starts to become almost constant on all the points of the slip zone. This phenomenon can be seen on Fig. 13 for a smooth and Fig. 14 for a rough surface.

One important difference between a rough and a smooth surface subjected to wear under partial slip conditions is that, for the rough surface, the increase of the contact area takes place much faster, but after a certain number of cycles it stays constant as for a smooth contact. In Fig. 15, the complete half-width of the contact can be seen, showing the evolution due to wear and Fig. 16 shows a zoom to the edge of the contact.

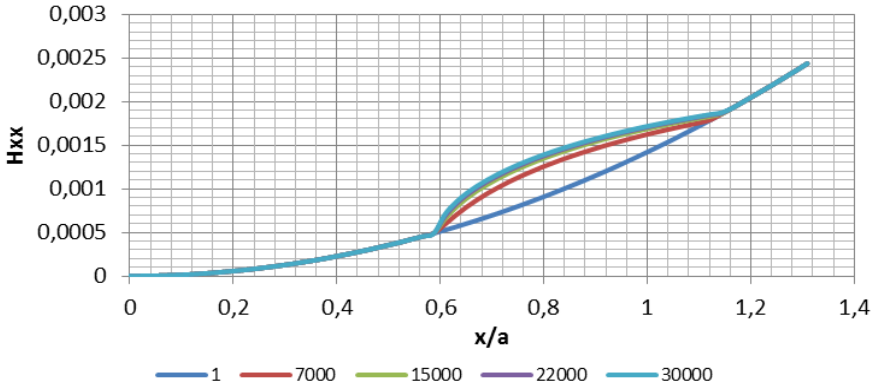

Fig. 10. Evolution of the gap due to wear in partial slip contact between a sphere and a half-space for a smooth surface (2D half)

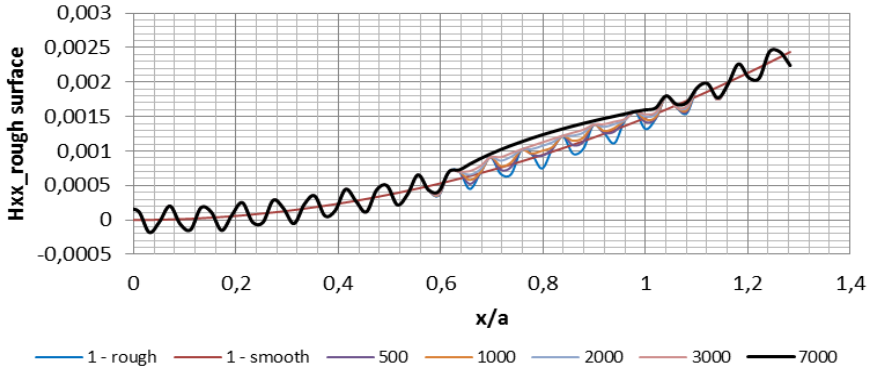

Fig. 11. Evolution of the gap due to wear in partial slip contact between a sphere and a half-space for a rough surface (2D half).

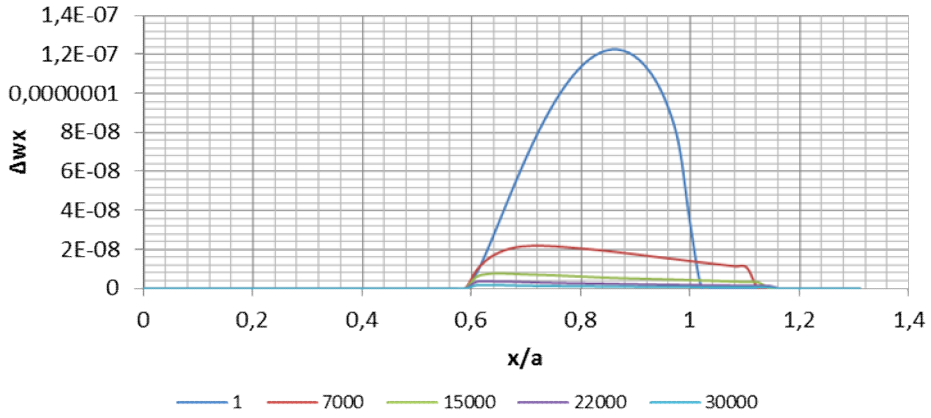

Fig. 13. Evolution of the wear values during one cycle on the slip area for a smooth surface (2D half)

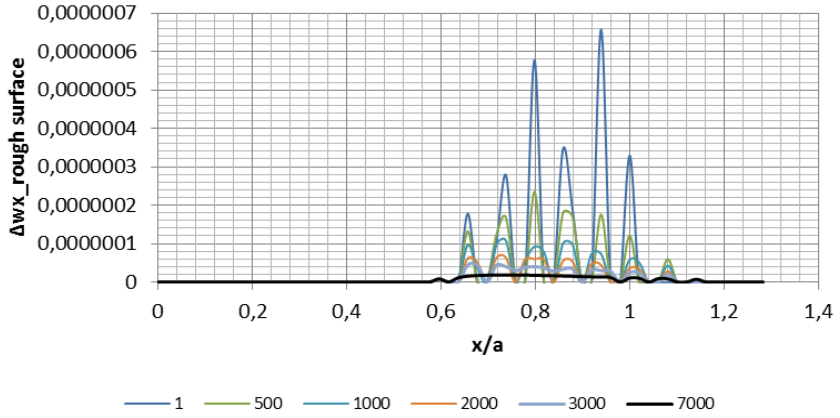

Fig. 14. Evolution of the wear values during one cycle on the slip area for a rough surface (2D half)

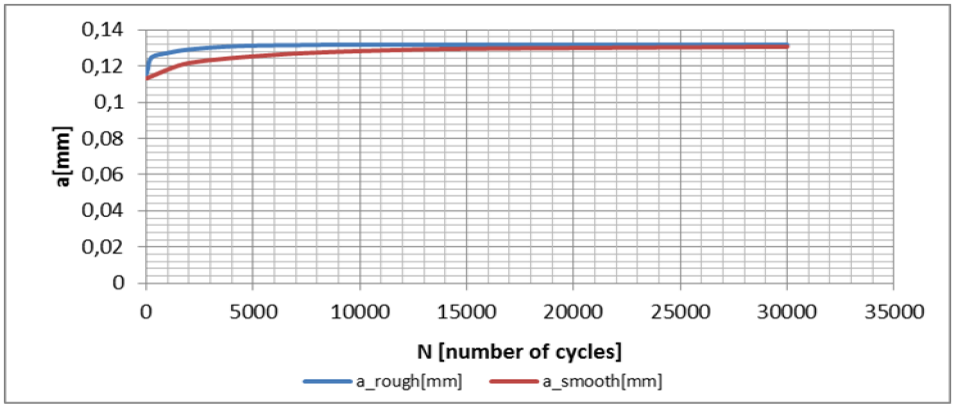

Fig. 15. Evolution of the half-contact width due to wear in partial slip contact between a sphere and a half-space (2D half) – complete half-width

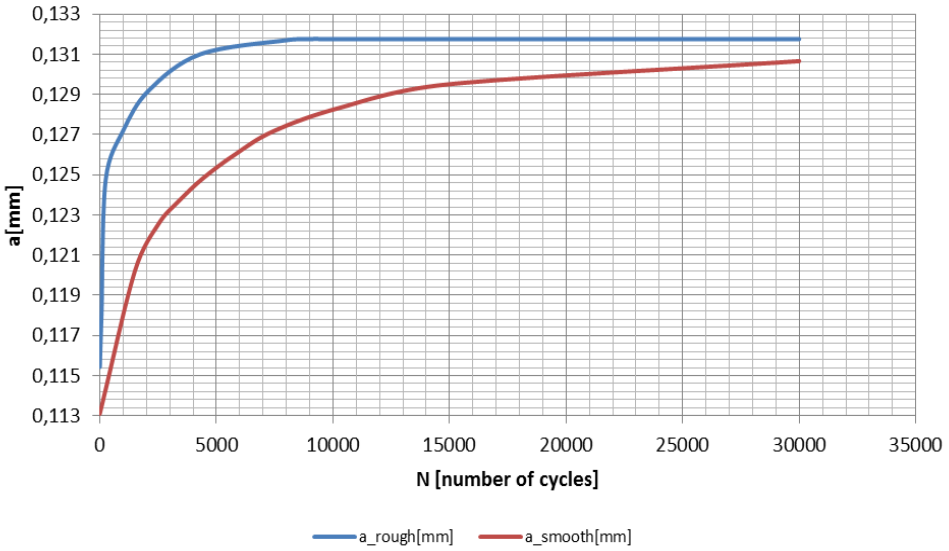

Fig. 16. Evolution of the half-contact width due to wear in a partial slip contact between a sphere and a half-space (2D half) – zoom to the edge of the contact.

4. CONCLUSION

Using analytical solutions from the literature, it was possible to create a numerical model to calculate the wear under partial slip conditions. The wear formation results in a high increase in the contact pressure, especially at the boundaries between stick and slip zones.

The wear is having higher values at the beginning of the wear process in the case of rough bodies in contact due to the high peaks of the pressure located on the top of each asperity. On a macro-scale, the results are comparable to a smooth surface profile and similarly on a micro-scale the pressure profile of each asperity behaves as a smooth surface. After a certain number of cycles, the behaviour on the slip zone is the same for smooth or rough bodies in contact. The increase of the half contact width takes place much faster for rough surfaces, but it stabilises almost at the same level.

The results from this study indicate that the effect of the wear is significant when investigating the contact pressures and the stresses and as well that the roughness of the contacting bodies is having an important role on the wear of mechanical components.

REFERENCES

1. **Archard J. F.,** 1953, Contact and rubbing of flat surfaces, *Journal of Applied Physics*, 24, pp. 981-988.
2. **Brun X. F., Melkote S. N.,** 2008, Modeling and experimental verification of partial slip for multiple frictional contact problems, *Wear*, 265, pp. 34-41.
3. **Cattaneo C.,** 1938, Sul contatto di due corpi elastici: distribuzione locale degli sforzi, Rend. Accad. Naz. Lincei, 27, pp. 342-348, 434-436, 474-478.
4. **Ciavarella M.,** 1998, The generalized Cattaneo partial slip plane contact problem. I-Theory, *Int. J. Solids Struct.*, 35 (18), pp. 2349-2362.
5. **Ciavarella M.,** 1998, The generalized Cattaneo partial slip plane contact problem. II-Examples, *Int. J. Solids Struct.*, 35 (18), pp. 2363-2378.

6. **Creţu S.,** 2009, Contactul concentrat elasto-plastic (Elasto-plastic concentrated contact) (in Romanian), Politehnium, Iași.
7. **Goryacheva I. G. et at.,** 2001, Wear in partial slip contact, *J. Tribol.*, 123, pp. 848-856.
8. **Hills D. A. et. at.,** 1994, Mechanics of Elastic Contacts, Butterworth-Heinemann. Oxford.
9. **Johansson L.,** 1994, Numerical Simulation of contact pressure evolution in fretting, *Journal of Tribology*, 116 (2), pp. 247-54.
10. **Johnson K. L.,** 1985, Contact Mechanics, Cambridge: Cambridge University Press.
11. **Kasarekar A. T. et. at.,** 2007, Modeling of fretting wear evolution in rough circular contacts in partial slip, *Int. J. of Mechanical Sciences*, 49, pp. 690-703.
12. **Kasarekar A. T. et. at.,** 2008, Fretting fatigue of rough surfaces, *Wear*, 264, pp. 719-730.
13. **Keer, L.M., Goodman, L.E.** 1976, Tangential loading of two bodies in contact, *J. Appl Mech.*, 42, pp. 513-514.
14. **Madge J. J. et. at.,** 2007, The critical role of fretting wear in the analysis of fretting fatigue, *Wear*, 263, pp. 542-551.
15. **Mindlin R. D.,** 1949, Compliance of elastic bodies in contact, *J. Appl. Mech.*, 16, pp. 259-268.
16. **Spence, D.A.** 1973, An eigenvalue problem for elastic contact with finite friction, *Proc. Cambridge Philosophical Society*, 73, pp. 249-268.
17. **Stowers I. F., Rabinowicz E.,** 1973, The mechanism of fretting wear, *Journal of Lubrication Technology*, 95, pp. 65-70.
18. **Truman C. E. et. at.,** 1995, Contact mechanics of wedge and cone indenters, *Int. J. Mech. Sci.*, 37 (3), pp. 261-175.